mologs. We present evidence that *SGT1b* has evolved a distinct capability in certain *R* gene–specified responses that is not compensated for by *SGT1a*. Nonredundant functions of *Arabidopsis* SGT1a and SGT1b in plant defense may reflect preferential interactions with different subsets of SCF complexes. Representation of at least 19 *SKP1* orthologs and >300 F-box–containing proteins in the *Arabidopsis* genome creates the potential for considerable flexibility in SCF composition and regulatory function (*16, 21–23*).

Our data show that *RAR1* and *SGT1b* each contribute quantitatively to *RPP5*-dependent resistance and are thus operationally distinct. It is noteworthy that Azevedo *et al*. (*15*) show conserved molecular association between plant SGT1 and RAR1, including *Arabidopsis* SGT1a and SGT1b. In barley extracts, SGT1 exists in two pools, one containing RAR1, the other engaging SCF components. The combined genetic and molecular data imply that SGT1-RAR1 and SGT1-SCF complexes have at least partially distinct roles in disease resistance. In one scenario, mutations in *RAR1* but not *SGT1a* or *SGT1b* might disable SGT1-RAR1 function, whereas mutations in *SGT1b* might compromise a subset of SCF complexes that are preferentially used in *R* gene–triggered responses. Such a model would account for the exclusive genetic requirements of certain *R* genes for either *RAR1* or *SGT1b*, directing signals through one or the other mechanism to trigger plant defense.

References and Notes

1. J. L. Dangl, J. D. G. Jones, *Nature* **411**, 826 (2001).
2. N. Inohara *et al*., *J. Biol. Chem*. **275**, 27823 (2000).
3. J. Cohn, G. Sessa, G. B. Martin, *Curr. Opin. Immunol*. **13**, 55 (2001).
4. J. E. Parker *et al*., *Plant Cell* **9**, 879 (1997).
5. See supplemental material on *Science* Online at www.sciencemag.org/cgi/content/full/1067747/DC1.
6. N. Aarts *et al*., *Proc. Natl. Acad. Sci. U.S.A*. **95**, 10306 (1998).
7. A. Falk *et al*., *Proc. Natl. Acad. Sci. U.S.A*. **96**, 3292 (1999).
8. D. Jirage *et al*., *Proc. Natl. Acad. Sci. U.S.A*. **96**, 13583 (1999).
9. B. J. Feys, L. J. Moisan, M. A. Newman, J. E. Parker, *EMBO J*. **20**, 5400 (2001).
10. P. Muskett *et al*., *Plant Cell*, in press.
11. J. H. Jørgensen, *Genome* **39**, 492 (1996).
12. K. Shirasu *et al*., *Cell* **99**, 355 (1999).
13. K. Kitegawa *et al*., *Mol. Cell* **4**, 21 (1999).
14. A positional cloning strategy was used to map three allelic, recessive mutations in *Arabidopsis* accession Landsberg *erecta* (Ler) to a 50-kb interval on the lower arm of chromosome 4 [bacterial artificial chromosome (BAC) F8L21] [Munich Information Center for Protein Sequences (MIPS) *Arabidopsis thaliana* Group, www.mips.biochem.mpg.de/proj/thal]. Direct DNA sequencing of candidate genes within this region identified mutations in a gene with homology to yeast *SGT1*, denoted *SGT1b* (GenBank accession number AF439976). There are two *SGT1* homologs in genomic DNA of *Arabidopsis* accession Columbia (Col-0) (www.mips.biochem.mpg.de/proj/thal). *SGT1a* (BAC F9D16; GenBank accession number AF439975) is linked by 6 Mb to *SGT1b* on chromosome 4. Ler *SGT1a* and *SGT1b* intron/exon structures were verified by sequencing genomic DNA. Ler and Col-0 SGT1b proteins are identical. Ler and Col-0 SGT1a differ by a single amino acid (residue 224). The presence of two Ler *SGT1* genes was confirmed on genomic DNA gel blots.
15. C. Azevedo *et al*., *Science* **295**, 2073 (2002); published online 14 February 2002 (10.1126/science.1067554).
16. The *Arabidopsis* Genome Initiative, *Nature* **408**, 796 (2000).
17. M. J. Austin *et al*., data not shown.
18. S. Lyapina *et al*., *Science* **292**, 1382 (2001).
19. R. J. Deshaies, *Annu. Rev. Cell Dev. Biol*. **15**, 435 (1999).
20. J. Callis, R. D. Vierstra, *Curr. Opin. Plant Biol*. **3**, 381 (2000).
21. M. A. Andrade, M. González-Guzmán, R. Serrano, P. L. Rodríguez, *Plant Mol. Biol*. **46**, 603 (2001).
22. R. Ferrás *et al*., *EMBO J*. **20**, 2742 (2001).
23. W. M. Gray, S. Kepinski, D. Rouse, O. Leyser, M. Estelle, *Nature* **414**, 271 (2001).
24. D. J. Kliebenstein *et al*., *Mol. Plant-Microbe Interact*. **12**, 1022 (1999).
25. J. D. Clarke, Y. Liu, D. F. Klessig, X. Dong, *Plant Cell* **10**, 557 (1998).
26. E. Koch, A. Slusarenko, *Plant Cell* **2**, 437 (1990).

27. Supported by the Gatsby Charitable Foundation, a BBSRC grant (J.P.), and an EMBO long-term fellowship (K.K.). We thank R. Last (Boyce Thompson Institute for Plant Research, Cornell University, Ithaca, NY) for antibody to PR1, and A. Sadanandom and K. Shirasu (Sainsbury Laboratory, Norwich, UK) for antibody to SGS.

5 November 2001; accepted 17 January 2002
Published online 14 February 2002;
10.1126/science.1067747
Include this information when citing this paper.

Structure of HP1 Chromodomain Bound to a Lysine 9–Methylated Histone H3 Tail

Steven A. Jacobs and Sepideh Khorasanizadeh*

The chromodomain of the HP1 family of proteins recognizes histone tails with specifically methylated lysines. Here, we present structural, energetic, and mutational analyses of the complex between the *Drosophila* HP1 chromodomain and the histone H3 tail with a methyllysine at residue 9, a modification associated with epigenetic silencing. The histone tail inserts as a β strand, completing the β-sandwich architecture of the chromodomain. The methylammonium group is caged by three aromatic side chains, whereas adjacent residues form discerning contacts with one face of the chromodomain. Comparison of dimethyl- and trimethyllysine-containing complexes suggests a role for cation-π and van der Waals interactions, with trimethylation slightly improving the binding affinity.

Although the structure of the nucleosome core particle is known, the histone tails, which protrude from the nucleosome core and undergo posttranslational modifications, have not been observed (*1*, *2*). A "histone code" hypothesis suggests that covalent modification of these tails, such as acetylation, phosphorylation, and methylation, creates a favorable docking surface for protein modules that interact with chromatin in a manner that may extend the genetic code (*3*). The sites of lysine methylation on histone tails have been known for 30 years, but direct evidence linking them to gene activity has only appeared recently. On histone H3, methylation at Lys^9 (MeK9 H3) produces a site for HP1 (heterochromatin-associated protein 1) binding, and is associated with epigenetic silencing in organisms as diverse as fission yeast and mammals (*4–8*). We recently showed that the chromodomain of *Drosophila* HP1 is sufficient for specific interactions with the histone H3 tail, in a manner that depends on the methylation of Lys^9 (*7*). Here, we show the structural and energetic determinants of this interaction to further elucidate the mechanism of methyllysine recognition, as well as histone H3 tail recognition by the chromodomain.

We used a pair of synthetic peptides corresponding to residues 1 to 15 of histone H3, which included dimethyllysine (Me_2K) and also trimethyllysine (Me_3K) at residue 9 (*9*). We used isothermal titration calorimetry to measure the affinity of the HP1 chromodomain for both Me_2K- and Me_3K-bearing peptides, and found these to be 7 and 2.5 μM, respectively (*9*). To visualize the chromodomain interaction with the H3 tail, we formed its complexes with these peptides and obtained crystals for x-ray diffraction studies. The structures were solved at 2.1 and 2.4 Å resolutions, respectively (*9*). Analysis of the $|2F_o - F_c|$ and $|F_o - F_c|$ difference maps clearly indicated electron density for the bound position of the H3 peptide in both complexes (Fig. 1A). We did not see residues 1 to 4 or 11 to 15 of the peptides, suggesting that only residues Gln^5-

Department of Biochemistry and Molecular Genetics, University of Virginia Health System, Charlottesville, VA 22908–0733, USA.

*To whom correspondence should be addressed. E-mail: khorasan@virginia.edu

Ser^{10} of histone H3 participate directly in binding to the chromodomain (*9*).

The overall conformation and binding topology of the H3 peptide on the chromodomain is shown in Fig. 1B. The structures involving the Me_2K9 and Me_3K9 peptides are essentially superimposable, with an overall root-mean-square deviation (rmsd) of 0.35 Å over all C^{α} atoms. The histone tail binds to only one face of the chromodomain, confirming our preliminary data obtained by solution nuclear magnetic resonance (NMR) spectroscopy (*7*). The insertion of the target peptide as a β strand is reminiscent of interactions seen in the PTB and PDZ domains with their recognition targets (*10*). In addition to an amino-terminal chromodomain, HP1 has a related carboxy-terminal chromo shadow domain. A structural comparison of the complex with the free chromodomain and the chromo shadow domain of HP1 is shown in Fig. 1B. NH_2-terminal residues do not form a β strand in the free chromodomain (*11*), suggesting that this β strand is induced on contact with the H3 tail peptide. Moreover, the β structure of the H3 tail was unanticipated, as its lack of detection in the nucleosome core particle structure suggested a disordered conformation (*1*, *2*).

It has been demonstrated that no combination of the naturally occurring amino acids gives rise to a motif that interacts with the HP1 chromodomain (*12*). This implies that the post translationally modified form of Lys^9 is absolutely required, consistent with our finding that, when all the H3 tail residues are included but without the methylation mark, there is no detectable binding (*7*). Similarly, a free methyllysine amino acid does not bind appreciably. Therefore, in describing the structure, it is useful to regard two distinct features of recognition: those involving the MeK and those involving the surrounding histone tail sequence. The MeK recognition involves a conserved aromatic pocket (Fig. 2A), whereas interactions between H3 tail and the chromodomain consist of a series of backbone hydrogen bonds and complementary surfaces formed between their side chains (Fig. 2B).

The disposition of the Me_2K and Me_3K within their binding environments is shown in Fig. 2A. The aromatic residues Tyr^{24}, Trp^{45}, and Tyr^{48} form a three-walled cage into which the methylammonium group inserts. Methylation of lysine changes two aspects of its chemistry. First, there is an increased hydrophobic property imparted to an otherwise polar terminal group. This would favor the propensity of van der Waals and hydrophobic interactions with nonpolar groups. Second, lysine methylation polarizes the C^{ε}-N^{ζ} bond, lending a more cationic character to the methylammonium group and leading to the stabilization of cation-π interactions with the aromatic cage (*13*, *14*).

Our calorimetry analyses (*9*) show that going from Me_2K to Me_3K produces a favorable gain of enthalpy ($\Delta\Delta H = -0.4$ kcal/mol) and entropy [$\Delta(T\Delta S) = 0.2$ kcal/mol] associated with chromodomain binding, consistent with improved interactions of a polar nature (i.e., cation-π interaction), in addition to the van der Waals contacts. Consistent with van der Waals interactions, the distance between the carbon atoms of the methyl groups and the centroids of the aromatic side chains fall within the range of 3.1 to 4.1 Å. In the structure of the dimethyllysine complex, there is an additional interaction with a water molecule 3.1 Å away, which is further buttressed by the side chain and backbone hydrogen bonding with Glu^{52} (Fig. 2A). In the Me_3K complex, the methylammonium group is no longer protonated, and the water molecule is displaced slightly away and out of hydrogen-bonding distance (3.8 Å). The water oxygen may participate in further side-chain polarization of the Me_2K, which is unnecessary in the Me_3K. In both cases, the methylammonium group is seated equidistant from each individual aromatic ring and occupies the focal point of the π-electron environment of the three aromatic residues.

To better assess the contribution of the chromodomain residues in Fig. 2A toward MeK recognition, we individually replaced these with alanine and measured the peptide binding affinity (Table 1 and Fig. 2C). Mutation of the aromatic cage residues, Tyr^{24}, Trp^{45}, and Tyr^{48}, reduces affinity for Me_3K9 H3 tail, dramatically. In contrast, changing the polar residues Glu^{23} and Glu^{52} to alanines results in a drop in affinity to less than one-half. This suggests that the aromatic cage plays a far more significant role in MeK binding than the nonaromatic residues. We also tested whether other long or hydrophobic side chains could replace the MeK9 within the aromatic cage. A Trp, Met, Leu, or an acetyllysine, when substituted for MeK9, results in the complete inability of the H3 tail to bind.

The bound portion of the H3 tail adopts a β strand conformation that lies antiparallel and coplanar with two chromodomain β regions, completing a three-stranded β sheet and the overall β-sandwich fold. Recognition of the MeK is only possible when presented in the correct context of the surrounding H3 sequence. Complementary surfaces stabilize the interactions between H3 tail and the chromodomain, burying a total of 1063 $Å^2$ of solvent-accessible

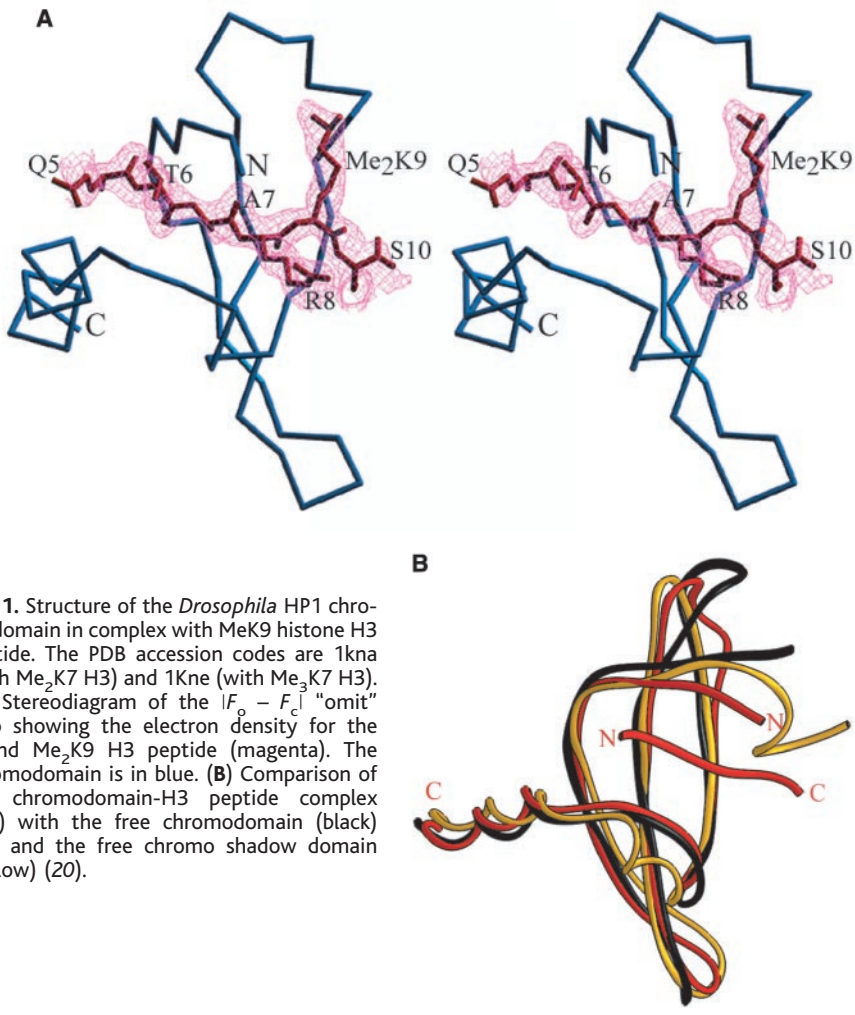

Fig. 1. Structure of the *Drosophila* HP1 chromodomain in complex with MeK9 histone H3 peptide. The PDB accession codes are 1kna (with Me_2K7 H3) and 1Kne (with Me_3K7 H3). (**A**) Stereodiagram of the $|F_o - F_c|$ "omit" map showing the electron density for the bound Me_2K9 H3 peptide (magenta). The chromodomain is in blue. (**B**) Comparison of the chromodomain-H3 peptide complex (red) with the free chromodomain (black) (*11*) and the free chromo shadow domain (yellow) (*20*).

surface area on both molecules as shown in Fig. 2B. This size compares favorably with other bona fide protein-protein interaction surfaces (*15*). Residues Gln[5], Thr[6], Ala[7], and Arg[8] of the H3 tail form β-sheet interactions with residues Glu[23], Tyr[24], Val[26], Asn[60], and Asp[62] in the chromodomain. In addition, the side chains of Thr[6] and Ala[7] form complementary van der Waals contacts, whereas Ser[10] forms hydrogen-bonded interactions with the chromodomain.

To better assess the contribution of each of the H3 tail residues shown in Fig. 2B toward chromodomain recognition, we prepared peptides with point mutations at each of these positions. The results are shown in Table 1 and Fig. 2D. The T6A mutation reduces the binding by a factor of 7 (*16*). This appears to be due to the partial loss of complementary interactions through the shortened side chain. It is noteworthy that the histone H3 tail contains a second sequence motif (AARK[27]S versus TARK[9]S) around Lys[27] (another known site of methylation) that differs only by this same Thr to Ala alteration. Consistent with our T6A mutagene-

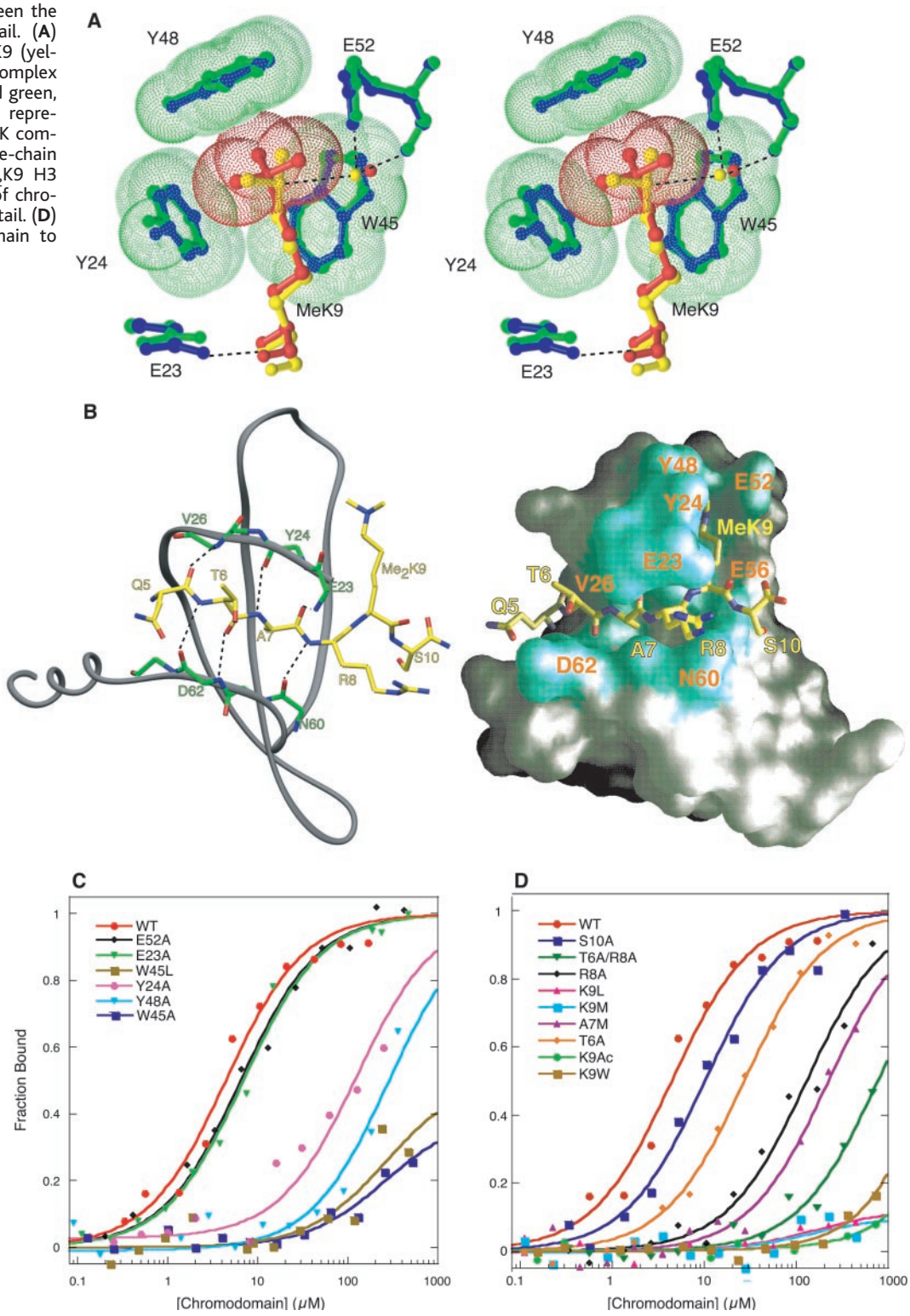

Fig. 2. Specific interactions between the chromodomain and MeK9 H3 tail. (**A**) Stereodiagram showing the Me_2K9 (yellow) and Me_3K9 (orange) H3 in complex with the chromodomain (blue and green, respectively). The van der Waals representation corresponds to the Me_3K complex. (**B**) Backbone (left) and side-chain (right) interactions between Me_2K9 H3 and chromodomain. (**C**) Binding of chromodomain mutants to Me_3K9 H3 tail. (**D**) Binding of wild-type chromodomain to point mutants of Me_3K9 H3 tail.

sis data, a peptide corresponding to H3 residues 15 to 32 bearing a methylated Lys[27] binds with an affinity one-seventh that of the methylated Lys[9] H3 peptide (*17*). This is also consistent with our structural finding that only the three side chains preceding and the one side chain following methylated lysine contribute to HP1 chromodomain binding specificity and suggests that the Lys[27] region is a second recognition site for the HP1 chromodomain.

Mutations of the other residues within the bound pentapeptide sequence further indicate their importance. Ala[7] makes intimate and complementary contacts with Val[26] of the chromodomain. The A7M mutation, which extends the size of the side chain and presumably leads to a steric clash, results in a reduction in binding by a factor of ~25. It is interesting that Val[26] of the chromodomain when mutated to a Met would similarly disturb the same interaction. We previously showed that V26M also results in the complete inability to support H3 binding (*7*). An R8A mutation in the peptide reduces the binding affinity by a factor of ~20. Finally, S10A mutation, which removes only an OH moiety, results in a drop in binding affinity by a factor of ~3. The examination of the crystal structures suggests a role for Ser[10] in forming a hydrogen bond interaction with Glu[56] of the chromodomain. HP1 chromodomain does not bind histone H3 containing methyllysine 4 (*7*), a posttranslational modification associated with transcriptional activation (*18*), because the sequence context of the Lys[4] (ARTK[4]Q) is not shared with Lys[9].

Table 1. Effect of point mutations (*16*) in the chromodomain and in the Me_3K9 H3 peptide. Data were obtained in 50 mM sodium phosphate (pH 8), 25 mM NaCl, and 2 mM dithiothreitol buffer at 15°C (*7*).

Chromo-domain	K_D (μM)	H3 peptide	K_D (μM)
Wild type	4 ± 1.0	K9M	>500
Mutants		K9W	>500
E23A	6.9 ± 0.9	K9L	>500
Y24A	>75	AcK9	>500
W45L	>500	R8A	>85
W45A	>500	A7M	>110
Y48A	>290	T6A	27 ± 4
E52A	6.5 ± 0.9	T6A/R8A	>500
		S10A	11.6 ± 3.5

A structure-based sequence alignment of chromodomains from diverse chromatin regulating factors is shown in Fig. 3, which indicates that MeK9 H3 binding is likely to be mediated by only a subset of the chromodomains. Category A shows chromodomains that contain the essential aromatic cage residues which in HP1 were observed to form the recognition pocket for MeK9. In addition, the majority of the chromodomains in subset A have most of the residues that in HP1 are responsible for H3 tail (Thr[6]-Ser[10]) sequence specificity. *Drosophila* PC and human SUV39H1 proteins have already been shown to interact with MeK9 H3 through pull-down assays (*5*). Sequences shown in category B have neither the complete aromatic cage nor the H3-discriminating residues of the HP1 chromodomain. These are likely to specify binding interactions with other target sequences and/or posttranslational modification. Consistent with this idea, we previously showed that the Esa1 chromodomain did not have specificity for MeK9 H3 tail (*7*). Moreover, the MOF chromodomain may bind to RNA rather than a protein (*19*). Finally, the chromo shadow domain of HP1, shown in category C, binds to the pentapeptide motif [PL][WRY]V[MIL][MLV] that does not share the H3 tail sequence or require MeK, but has been seen in nonhistone proteins that interact with HP1 (*12*, *20*). This would be consistent with the lack of sequence conservation in the cage and the peptide binding sites with respect to the chromodomain of HP1. Together, these analyses suggest that considerable diversity of recognition could be generated within the chromodomain family through relatively few amino acid substitutions at the aromatic cage or the peptide-binding sites.

The structure of the chromodomain complex presented here illustrates for the first time two features likely to be shared by other MeK recognition factors. The first is a distinct aromatic cage environment for the recognition of the cationic and hydrophobic methylammonium functionality. The second is an extended surface groove that distinguishes the sequence context of the MeK by forming additional interactions with the adjacent residues of the histone tail. HP1 homodimerizes solely through the chromo shadow domain, which does not interact with the chromodomain (*7*, *20*). Therefore, it would appear likely that one dimeric HP1 binds to Lys[9] and Lys[27] regions of a single H3 tail using its two monomeric chromodomains. Alternatively, a dimeric HP1 may bind to Lys[9] on two adjacent H3 tails. These and other hypotheses remain to be tested through additional biochemical and structural studies.

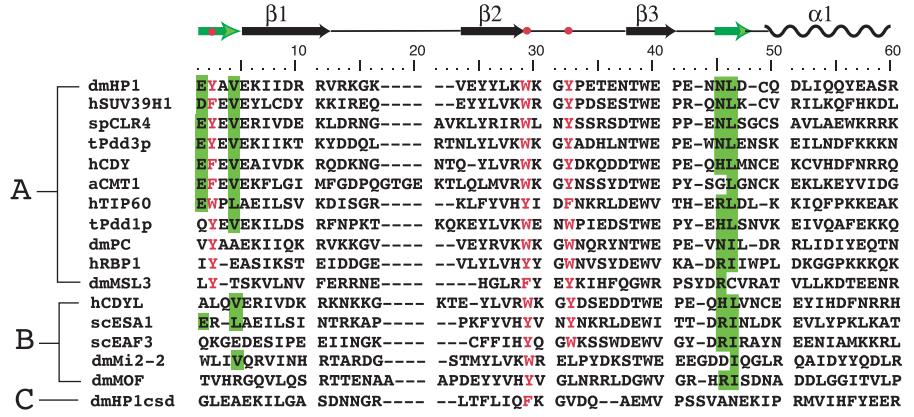

Fig. 3. Structure-based sequence alignment and organization of the chromodomains. Abbreviations are dm for *Drosophila*, h for human, sp for *Schizosaccharomyces pombe*, t for *Tetrahymena*, a for *Arabidopsis*, and sc for *Saccharomyces cerevisiae*. Aromatic cage residues that recognize MeK9 are in red. Conserved residues that form a complementary surface responsible for H3 peptide recognition are highlighted in green; arrows indicate β strands.

References and Notes

1. J. M. Harp, B. L. Hanson, D. E. Timm, G. J. Bunick, *Acta Cryst.* **D56**, 1513 (2000).
2. K. Luger, A. W. Maeder, R. K. Richmond, D. F. Sargent, T. J. Richmond, *Nature* **389**, 251 (1997).
3. T. Jenuwein, C. D. Allis, *Science* **293**, 1074 (2001).
4. A. J. Bannister *et al.*, *Nature* **410**, 120 (2001).
5. M. Lachner, D. O'Carroll, S. Rea, K. Mechtler, T. Jenuwein, *Nature* **410**, 116 (2001).
6. J.-i. Nakayama, J. C. Rice, B. D. Strahl, C. D. Allis, S. I. S. Grewal, *Science* **292**, 110 (2001).
7. S. A. Jacobs *et al.*, *EMBO J.* **20**, 5232 (2001).
8. S. J. Nielsen *et al.*, *Nature* **412**, 561 (2001).
9. Supplementary data are available on *Science* Online at www.sciencemag.org/cgi/content/full/1069473/DC1.
10. J. Kuriyan, D. Cowburn, *Annu. Rev. Biophys. Biomol. Struct.* **26**, 259 (1997).
11. L. J. Ball *et al.*, *EMBO J.* **16**, 2473 (1997).
12. J. F. Smothers, S. Henikoff, *Curr. Biol.* **10**, 27 (2000).
13. S. D. Black, D. R. Mould, *Anal. Biochem.* **193**, 72 (1991).
14. J. P. Gallivan, D. A. Dougherty, *Proc. Natl. Acad. Sci. U.S.A.* **96**, 9459 (1999).
15. J. Janin, S. Miller, C. Chothia, *J. Mol. Biol.* **204**, 155 (1998).
16. Single-letter abbreviations for the amino acid residues are as follows: A, Ala; C, Cys; D, Asp; E, Glu; F, Phe; G, Gly; H, His; I, Ile; K, Lys; L, Leu; M, Met; N, Asn; P, Pro; Q, Gln; R, Arg; S, Ser; T, Thr; V, Val; W, Trp; and Y, Tyr.
17. S. A. Jacobs, S. Khorasanizadeh, unpublished observations.
18. B. D. Strahl, R. Ohba, R. G. Cook, C. D. Allis, *Proc. Natl. Acad. Sci. U.S.A.* **96**, 14967 (1999).
19. A. Akhtar, D. Zink, P. B. Becker, *Nature* **407**, 405 (2000).
20. S. V. Brasher *et al.*, *EMBO J.* **19**, 1584 (2000).

21. We thank F. Rastinejad for access to the Pharmacology X-Ray Diffraction Laboratory, C. D. Allis for continued support and encouragement, and M. F. Summers for access to an isothermal titration calorimetry instrument. Peptide synthesis was supported by grant GM63959-01 to C. D. Allis.

2 January 2002; accepted 8 February 2002
Published online 21 February 2002;
10.1126/science.1069473
Include this information when citing this paper.